



## A novel mechanism for NLRP3 inflammasome activation

Tan Zhang<sup>a,b,c,d</sup>, Jingyao Zhao<sup>b</sup>, Tiemin Liu<sup>e</sup>, Wei Cheng<sup>f,\*\*</sup>, Yibing Wang<sup>a,d,\*\*\*</sup>,  
Shuzhe Ding<sup>c,\*\*\*\*</sup>, Ru Wang<sup>a,d,\*</sup>

<sup>a</sup> School of Kinesiology, Shanghai University of Sport, Shanghai, 200438, China

<sup>b</sup> Department of Microbiology & Immunology, College of Physicians & Surgeons, Columbia University, New York, NY, 10032, USA

<sup>c</sup> Key Laboratory of Adolescent Health Assessment and Exercise Intervention, Ministry of Education, East China Normal University, Shanghai, 200241, China

<sup>d</sup> Shanghai Frontiers Science Research Base of Exercise and Metabolic Health, Shanghai, 200438, China

<sup>e</sup> State Key Laboratory of Genetic Engineering, School of Life Sciences, Human Phenome Institute, Shanghai Key Laboratory of Metabolic Remodeling and Health, Institute of Metabolism & Integrative Biology, Zhongshan Hospital, Fudan University, Shanghai, 200438, China

<sup>f</sup> Department of Endocrinology, Yangpu Hospital Affiliated to Tongji University, Shanghai, 200090, China

### ARTICLE INFO

#### Keywords:

NLRP3 inflammasome  
Mitochondria  
mtDNA  
K<sup>+</sup> efflux  
Tfam

### ABSTRACT

The NLRP3 inflammasome, as an important component of the innate immune system, plays vital roles in various metabolic disorders. It has been reported that the NLRP3 inflammasome can be activated by a broad range of distinct stimuli, such as K<sup>+</sup> efflux, mitochondrial dysfunction, lysosomal disruption and trans-Golgi disassembly, etc. However, there has been no well-established model for NLRP3 inflammasome activation so far, especially the underlying mechanisms for mitochondria in NLRP3 inflammasome activation remain elusive. Given that K<sup>+</sup> efflux is a widely accepted nexus for triggering activation of NLRP3 inflammasome in most previous studies, we sought to elucidate the role of mitochondria in K<sup>+</sup> efflux-induced NLRP3 inflammasome activation. Here, we demonstrated that inflammation activation by LPS evoked the expression of genes that involved in mitochondrial biogenesis and mitophagy, subsequently mitochondrial mass and mitochondrial membrane potential were also elevated, suggesting the contribution of mitochondria in inflammatory responses. Moreover, we inhibited mitochondrial biogenesis by silencing Tfam and genetic ablation of Tfam abolished the NLRP3 inflammasome activation induced by K<sup>+</sup> efflux via release of mitochondrial DNA (mtDNA), as deprivation of cellular mtDNA by EtBr treatment could reverse inflammasome activation induced by K<sup>+</sup> efflux. Collectively, we reveal that mtDNA release induced by K<sup>+</sup> efflux in macrophages activates NLRP3 inflammasome, and propose that mitochondria may serve as a potential therapeutic target for NLRP3 inflammasome-related diseases.

### 1. Introduction

The innate immunity is the first line of defense against pathogens and cellular damage that recognizes infection and detects non-self molecules, while pathogen-associated molecular patterns (PAMPs) derived from pathogens or damaged-associated molecular patterns (DAMPs) from host-derived molecules are sensed via distinct pattern recognition receptors (PRRs), which are located in the cytoplasm or on the plasma membrane of the host cells [1]. Among a variety of PRRs identified, Nucleotide-binding oligomerization domain, leucine rich repeat and

pyrin domain containing 3 (NLRP3) inflammasome is an intracellular multiple protein complex that is consisted of the sensor protein NLRP3, the adaptor apoptosis-associated speck-like protein (ASC) and the effector protein caspase-1 [2]. Aberrant activation of NLRP3 inflammasome abnormally upregulates pro-inflammatory cytokines and thus is engaged in the pathogenesis of various inflammatory diseases, including cryopyrin-associated periodic syndrome (CAPS) [3], cancer [4]. Moreover, inflammation has been identified as one of the critical driving forces of various metabolic disorders [5], including obesity [6], type 2 diabetes [7], non-alcoholic fatty liver disease (NAFLD) [8], gout [9],

\* Corresponding author. School of Kinesiology, Shanghai University of Sport, Shanghai 200438, China.

\*\* Corresponding author.

\*\*\* Corresponding author. School of Kinesiology, Shanghai University of Sport, Shanghai 200438, China.

\*\*\*\* Corresponding author.

E-mail addresses: [chengwei780411@sohu.com](mailto:chengwei780411@sohu.com) (W. Cheng), [wangyibing@sus.edu.cn](mailto:wangyibing@sus.edu.cn) (Y. Wang), [szding@tyxx.ecnu.edu.cn](mailto:szding@tyxx.ecnu.edu.cn) (S. Ding), [wangru@sus.edu.cn](mailto:wangru@sus.edu.cn) (R. Wang).

<https://doi.org/10.1016/j.metop.2022.100166>

Received 29 December 2021; Received in revised form 19 January 2022; Accepted 20 January 2022

Available online 22 January 2022

2589-9368/© 2022 Published by Elsevier Inc. This is an open access article under the CC BY-NC-ND license (<http://creativecommons.org/licenses/by-nc-nd/4.0/>).

atherosclerosis [10] and neurodegenerative diseases as well [11]. Given the crucial role of NLRP3 inflammasome in governing inflammation, metabolic and immune diseases, elucidating the mechanisms underlying NLRP3 inflammasome activation warrants development of novel and promising therapeutic approaches to combat these disorders.

In general, NLRP3 activation includes two stages: “priming” and “activation” [12]. Priming stage involves the engagement of PRRs, such as Toll-like receptors (TLRs) that respond to PAMPs or DAMPs, such as LPS, and leading to nuclear factor- $\kappa$ B (NF- $\kappa$ B) activation, subsequently resulted in enhanced transcription expression of inflammatory interleukin-1  $\beta$  (IL-1 $\beta$ ), interleukin-18 (IL-18) and NLRP3. The mechanism of “activation” stage has remained relatively obscure so far. Upon stimulation, NLRP3 is oligomerized and then recruits and interacts with ASC via its N-terminal pyrin domain (PYD) in NLRP3 [13]. Subsequently, the bound ASC further recruits caspase-1, primes self-cleavage and activation of mature caspase-1 which then elevated production of the pro-inflammatory cytokines, IL- $\beta$  and IL-18 through proteolytic cleavage.

Although the ‘activation’ stage of NLRP3 inflammasome is elicited by a variety of irrelevant stimuli, including intracellular ion flux [14–18], lysosomal damage [19], mitochondrial dysfunction [20] and metabolic regulation [12,21], the precise mechanism responsible for NLRP3 inflammasome activation has been poorly deciphered due to the extremely diversified structures and sources of these activators. Of note, mitochondria have been reported to play a pivotal role in NLRP3 inflammasome activation. Mitochondrial genome is unique and replicates independent of nuclear genome, which is named as mitochondrial DNA (mtDNA). Recent studies have indicated that mtDNA, which belongs to the intracellular DAMPs, is released into cytoplasm after mitochondrial damage, and concomitantly activates NLRP3 inflammasome by direct engagement [22,23]. Nevertheless, some other studies have shown that mitochondria may not be involved in NLRP3 inflammasome activation [24]. Therefore, the role of mitochondria during NLRP3 inflammasome activation is controversial and needs to be clarified. In addition, among all the NLRP3 stimuli,  $K^+$  efflux is a well-established mediator that facilitating NLRP3 activation in response to numerous NLRP3 activators, such as ATP, crystalline substance and bacterial toxins, as all of the above stimuli trigger  $K^+$  efflux in murine macrophages [14]. Although both  $K^+$  efflux and mitochondria pathways mediate NLRP3 inflammasome activation, how these two signaling pathways coordinate with each other during NLRP3 inflammasome activation remains largely unclear.

In this study, we first found that inflammation activation induced the expression of genes involved in mitochondrial biogenesis and mitophagy, eliciting gradual increases in mitochondrial mass and mitochondrial membrane potential, and suggested an involvement of mitochondria in inflammatory responses. Mechanistically, we inhibited mitochondrial biogenesis by silencing transcription factor A, mitochondrial (Tfam). Tfam is the nuclear DNA (nDNA)-encoded protein which translocates to mitochondria and binds to mtDNA to promote its compaction, thus playing a crucial role in replication and transcription of mtDNA [25]. Our results revealed that Tfam silencing diminished NLRP3 inflammasome activation and cytosolic release of mtDNA induced by  $K^+$  efflux, implying that to certain extent, mitochondria may mediate NLRP3 inflammasome activity through the cytosolic release of mtDNA. Next, to verify the role of mtDNA in mediating function of NLRP3 inflammasome, we treated macrophages with ethidium bromide (EtBr) to deplete mtDNA and confirmed that the NLRP3 inflammasome activation induced by  $K^+$  efflux was markedly reduced by mtDNA depletion. Taken together, we have delineated a novel mechanism for NLRP3 inflammasome activation that the cytosolic release of mtDNA induced by  $K^+$  efflux in macrophages activates NLRP3 inflammasome,

arguing for mitochondria as a potential therapeutic target for NLRP3 inflammasome-related diseases, such as obesity [6], type 2 diabetes [7], NAFLD [8], gout [9], atherosclerosis [10] and neurodegenerative diseases [11].

## 2. Materials and methods

### 2.1. Cell culture

L929 (ATCC, CCL-1) cells and J774A.1 macrophages (ATCC, TIB-67) were obtained from American Type Culture Collection, 293FT cells (ThermoFisher Scientific, R70007) were obtained from ThermoFisher Scientific and are putatively of female origin,  $\psi$ CREJ2 cells (a kind gift from Prof. KA Fitzgerald) were used to produce J2 v-myc/v-raf transforming retrovirus. Cell lines were cultured in Dulbecco’s modified Eagle’s medium (DMEM) supplemented with 10% fetal bovine serum (FBS, Gibco, 10,099–141), penicillin (100 U/ml) and streptomycin (100  $\mu$ g/ml).

L929 conditioned media was prepared from the supernatant of a 7-day culture of L929 cells. Supernatant was harvested and clarified by centrifugation at 1500 rpm for 5 min at room temperature and then filtered. Bone marrow derived macrophages (BMDMs) were harvested from 8- to 12-week-old C57BL/6 mice as previously described [26]. For BMDMs immortalization, supernatant from  $\psi$ CREJ2 cells was filtered and then added to BMDMs at day 1 for 16–24 h. Macrophages were washed with 1xPBS buffer and allowed to rest for an additional 16–24 h. Then, a second round of infection was repeated. BMDMs were incubated in DMEM containing 10% FBS, penicillin (100 U/ml), streptomycin (100  $\mu$ g/ml) and 30% L929 conditioned media for a few weeks, immortalized BMDMs (IBMMs) were grown in DMEM added with 10% FBS, penicillin (100 U/ml), streptomycin (100  $\mu$ g/ml) and 10% L929 conditioned media [26].

### 2.2. Reagents

LPS (*E.coli* 026:B6) and ATP (A1852) were obtained from Sigma-Aldrich. MitoTracker Green<sup>FM</sup> (M7514) and MitoTracker Deep Red<sup>FM</sup> (M22426) were purchased from Invitrogen. Antibody against Tfam (Sc-166,965) was obtained from Santa Cruz Biotechnology. Antibody against NLRP3 (AG-20B-0014-C100) were obtained from AdipoGen. Antibody against IL-1 $\beta$  (AF-401-NA) was obtained from R&D Systems. Antibody against GAPDH (10R-G109a) was obtained from Fitzgerald. Antibody against TOM20 (HPA011562) was obtained from Sigma-Aldrich. Alexa Fluor 488 Donkey anti-mouse IgG (A-21202) and Alexa Fluor 594 donkey anti-rabbit IgG (A-21207) were obtained from Invitrogen.

### 2.3. Inflammasome stimulation

To induce NLRP3 inflammasome activation, IBMMs or J774A.1 macrophages were plated on 6- or 12-well plates and allowed for growth overnight. On day 2, the cells were either vehicle-treated or incubated with LPS (100 ng/ml) for 4 h and primed for induction of NF- $\kappa$ B-dependent increases in pro-IL-1 $\beta$  and NLRP3 expression and then the cell culture medium was removed and replaced with fresh culture medium (140 mM NaCl, 5 mM KCl, 1.3 mM CaCl<sub>2</sub>, 1.0 mM MgSO<sub>4</sub>, 10 mM HEPES (pH7.5), 5.5 mM glucose) or  $K^+$ -free media (145 mM NaCl, 1.3 mM CaCl<sub>2</sub>, 1.0 mM MgSO<sub>4</sub>, 10 mM HEPES (pH7.5), 5.5 mM glucose) in which  $K^+$  was replaced by Na<sup>+</sup> for 2 h [24].

#### 2.4. Lentivirus generation and IBMMs transduction

The shRNA sequences are as follows: shTfam64 5'-CCGGGCTGAG TGGAAAGCA TACAACTCGAGTTTGTATGCTTCCACTCAGCTTTTGTG-3'; shTfam65 5'-CC-

GGCGTCTATCAGTCTTGTCTGTACTCGAGTACAGACAAGACTGATA GACGTTTTTG-3'; shTfam66 5'-CCGGCGGAGACATCTCTGAGCATTAC TCGAGTAATG.

CTCAGAGATG TCTCCGTTTTTG-3; shCtrl 5'-CCGGCAACAAGATG AAGAGC.

ACCAACTCGAGTTGGTCTCTTCATCTTGTGTTTTTG-3'. These oligos were annealed in PCR cyclers to synthesize the double-strand DNA (dsDNA). The pLKO.1 vector (Addgene plasmid #8453) was digested by AgeI and EcoRI restriction enzymes, and then ligated with the dsDNA. The generation of lentivirus and IBMMs transduction were conducted as previously described [26]. Briefly, 293FT cells were transfected with pLKO.1 containing shCtrl or shTfam sequences in combination with package vector psPAX2 (Addgene plasmid #12260) and envelop vector pCMV-VSV-G (Addgene plasmid #8454) using FUGENE 6 reagent as the transfection reagent (Promega, E2691). Medium of 293FT cells was changed 6 h after transfection and replaced with 10 ml fresh culture media. At 48 h post-transfection, the supernatant containing lentiviral particles was collected, centrifuged at 1500 rpm for 5 min and then filtered through 0.45 µm filter. 10 ml new media was added to 293FT cells and supernatant was collected, centrifuged and filtered 72 h post-transfection. 500,000 of IBMM cells were transduced with 1 ml crude lentiviral particles, 6 µg/ml polybrene (Sigma, TR-1003-G) and 10 mM HEPES (Sigma, H3375) by spinfection at 1800 rpm 27 °C for 90 min in non-treated 12-well plate. 1 ml lentiviral particles were added and spinfection was repeated the following day. 48 h post first transduction, IBMMs were replaced with fresh culture media and selected with 4 µg/ml puromycin for 4 days. The knockdown efficiency of Tfam was validated by qRT-PCR and immunoblot analysis.

#### 2.5 Flow Cytometry.

To measure mitochondrial mass and mitochondrial membrane potential, IBMMs were plated on 12-well plates at 150,000 cells/well overnight. On day 2, cells were vehicle-treated or treated with LPS (100 ng/ml) for indicated times, and stained with 50 nM MitoTracker Green and MitoTracker Deep Red for 30 min at 37 °C [26]. Mitochondrial mass and mitochondrial membrane potential were detected by flow cytometry on a Fortessa cytometer (BD). Data analysis was performed using FlowJo software and background fluorescence from unstained controls was subtracted from respective stained samples.

#### 2.6 RNA Isolation and qRT-PCR.

Total RNA was extracted from cells by using Rneasy mini kit (Qiagen). The quality and quantity of RNA were determined by photometry (Gen5 BioTek). For cDNA synthesis, 2 µg RNA were reverse transcribed to cDNA using Superscript III enzyme and oligo dT (Invitrogen). qPCR was performed using SYBR Green mix and primer sequences are shown as follows: Tfam Forward (5'-3'):GGAATGTGGAGCGTGCT.

AAAA, Reverse (5'-3'): ACAAGACTGATAGACGAGGGG; PGC-1α Forward (5'-3')

):AGGCCCGTGTGA TTTACGTT, Reverse (5'-3'): CCGCAGATTTAC GGTGCAT.

T; NRF-1 Forward (5'-3'):ACAGATAGTCCTGTCTGGGGAAA, Reverse (5'-3'): TGGTACATGCTCACAGGGATCT; NRF2 Forward (5'-3'): CTTT AGTCAGCGAC.

AGAAGGAC, Reverse (5'-3'): AGGCATCTTGTGGGAATGTG; PI NK1 Forward (5'-3'): TTCTCCGCCAGTCGGTAG, Reverse (5'-3'): CTG CTTCTCCTCGATCA.

GCC; Parkin Forward (5'-3'): TCTTCCAGGTAACCACCGTC, Reverse (5'-3'): GGCAGGGAGTAG CCAAGTT; Atg 7 Forward (5'-3'): GTTCG CCCCCTTAATA.

GTGC, Reverse (5'-3'): TGAAGTCCAACGTCAGCGG; LC3b Forward (5'-3'): AGTGAAGATGTCCGGCTCA, Reverse (5'-3'): GTGGTCAGG CACCAGGAAC.

T; Hprt Forward (5'-3'):GTTAAGCAGTACAGCCCCAAA, Reverse (5'-3'): AGG.

GCATATCCAACAACAACTT. Differences in cDNA inputs were normalized to Hprt cDNA levels. Relative quantitation of target cDNA was determined by formula  $2^{-\Delta\Delta CT}$ .

#### 2.5. Measurement of mtDNA copy number

Measurement of copy number of total mtDNA was previously described [26]. Total DNA was isolated from cells using the DNeasy Blood & Tissue Kit (Qiagen). DNA concentrations were detected by photometry (Gen5 Bio Tek). 15 ng, 7.5 ng and 3.75 ng DNA were used to conduct qPCR for mitochondrial gene mtCOI and nuclear gene ndufv1. The primer sequences are as followed: mtCOI Forward (5'-3'): TGCTAGCCGAGGCATTAC, Reverse (5'-3'): GGGTGCCCAAAGAATCA-GAAC; Ndufv1 Forward (5'-3'): CTTCCCCTGGCCTCAAG, Reverse (5'-3'): CCAAACCCAGTGACCAGC; Ratios of  $2^{-\Delta\Delta CT}$  for mtCOI over Ndufv1 for the different DNA concentrations were averaged.

The copy number of cytosol mtDNA was measured as previously described [22]. Briefly,  $1 \times 10^7$  cells were homogenized with Douncer in 100 mM Tricine-NaOH solution, pH 7.4 containing 0.25 M sucrose, 1 mM EDTA and protease inhibitor, and centrifuged at 700 g for 10 min at 4 °C. The protein concentration and volume of the supernatant was normalized, followed by centrifugation at 10,000 g for 30 min at 4 °C to produce the supernatant (cytosolic fraction). DNA was isolated from 200 µl of the cytosolic fraction as described above. Copy number of mtCOI DNA was measured by quantitative real time PCR using same volume of the DNA solution.

#### 2.6. Western Blot

Cells were washed with 1xPBS buffer and then lysed in Triton lysis buffer (1% Triton X-100, 150 mM NaCl, 50 mM HEPES, 5 mM EDTA, pH 7.5) with 1 mM DTT and protease inhibitor (1 mM PMSF, 1 µg/ml aprotinin, 10 µg/ml pepstatin and 1 µg/ml leupeptin) and incubated on ice for 20 min. Lysates were then centrifuged at 15,000 rpm for 15 min at 4 °C. Total cell lysates were resolved by SDS-PAGE and analyzed for IL-1β protein levels. To examine secreted IL-1β, culture medium was collected, equal volume of methanol and 1/4 volume of chloroform were added and vortex mixed to precipitate the proteins. The mixtures then were centrifuged at 12,000 rpm at 4 °C for 10 min, the upper layer was discarded, the bottom layer was transferred to a new tube and equal volume of methanol was added and vortex mixed. The mixtures were centrifuged at 12,000 rpm at 4 °C for 10 min, the supernatant was discarded and the pellet was dried at 55 °C for 5 min, then 1xloading buffer was added to the pellet and then boiled at 95 °C for 5 min. The cell culture medium lysates were resolved by SDS-PAGE and analyzed for IL-1β protein levels.

Protein concentration was determined using the microBCA protein kit (Thermo Scientific). 20–40 µg total lysate was separated by SDS-PAGE and transferred onto a PVDF membrane. Membranes were blocked with 5% non-fat milk in TBST and then incubated with primary and secondary antibodies, respectively. ECL Western Blotting Detection Reagents (GE Healthcare), Super Signal West Pico Plus Chemiluminescent Substrate (Thermo Fisher) and Luminata Forte Western HRP Substrate (Millipore) were used for development of protein bands.

#### 2.7. ELISA

Cells were plated on non-treated 6-well plates at 300,000 cells/well and allowed for growth overnight. On day 2, cells were vehicle-treated or primed with LPS (100 ng/ml) for 4 h, followed by incubation with regular culture medium containing 5 mM K<sup>+</sup> or K<sup>+</sup>-free media in which K<sup>+</sup> was replaced by Na<sup>+</sup> for 2 h. Supernatant was collected and clarified and cytokine levels were determined with mouse IL-1β ELISA kits (BD Biosciences) following the manufacturer's protocol.

2.8. Generation of mitochondrial DNA deficient cells ( $\rho 0$  J774A.1)

J774A.1 macrophages were grown in DMEM supplemented with 10% FBS, penicillin (100 U/ml) and streptomycin (100  $\mu$ g/ml). Different

concentrations of EtBr (Sigma, E1510) were added to the medium for 2 weeks to generate  $\rho 0$  J774A.1 macrophages as previously described [22].  $\rho 0$  J774A.1 macrophages were cultured with DMEM supplemented with 10% FBS, penicillin (100 U/ml), streptomycin (100  $\mu$ g/ml), sodium

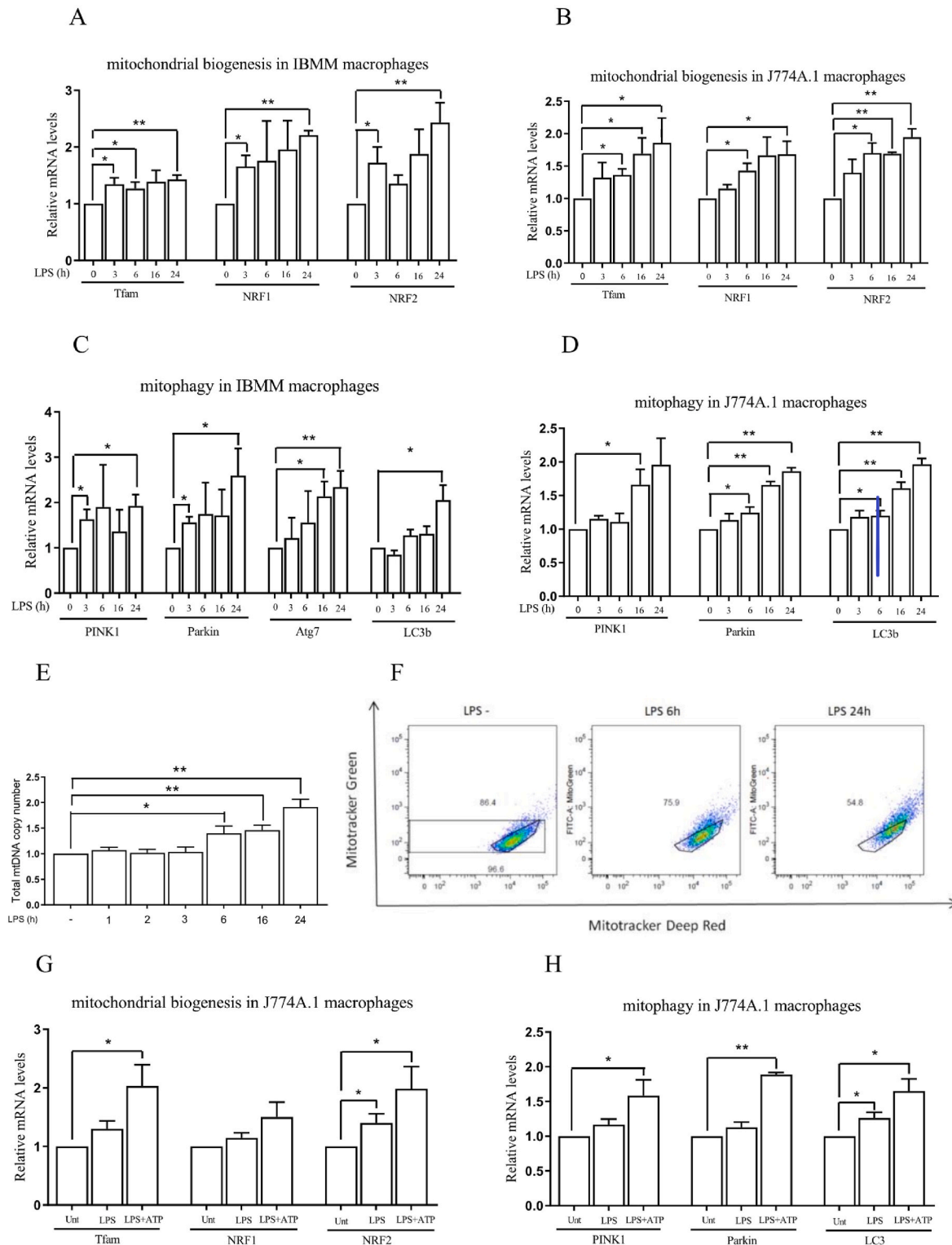


**Fig. 1.** Inflammatory state in vitro induced by LPS treatment leads to mitochondrial network expansion in macrophages. **A, B:** IBMMs and J774A.1 macrophages were vehicle-treated or treated with LPS (100 ng/ml) for indicated times, then the mRNA levels of genes involved in mitochondrial biogenesis were measured, **C, D:** Mitophagy were measured by qRT-PCR. **E:** Total mtDNA copy number in IBMMs was assessed by qPCR. **F:** Mitochondrial mass and mitochondrial membrane potential in IBMMs were detected by flow cytometry. **G, H:** J774A.1 macrophages were vehicle-treated or primed with LPS for 4 h, then incubated with ATP (4 mM, 1 h). The mRNA levels of genes involved in mitochondrial biogenesis and mitophagy were measured by qRT-PCR. n = 3, \*P < 0.05, \*\*P < 0.01.

pyruvate (100 µg/ml) and uridine (50 µg/ml).

### 2.9. Detection of intracellular K<sup>+</sup> concentration

Intracellular K<sup>+</sup> concentration was measured using the Potassium turbidimetric Assay Kit following manufacturer's guideline (Elabscience, E-BC-K279-M).

### 2.10. Confocal microscopy

Cells were plated on glass slides and allowed for growth overnight. On day 2, cells were vehicle-treated or primed with LPS (100 ng/ml) for 4 h, followed by incubation with regular culture medium containing 5 mM K<sup>+</sup> or K<sup>+</sup>-free media in which K<sup>+</sup> was replaced by Na<sup>+</sup> for 2 h. After stimulation, cells were washed with 1xPBS buffer and then fixed with

4% paraformaldehyde for 10 min, followed by permeabilization with 0.1% Triton-X-100 for 10 min. Cells were then blocked with 10% donkey serum in 1xPBS buffer and subsequently incubated with primary antibodies overnight at 4 °C, followed by incubation with Alexa Fluor secondary antibodies for 60 min at room temperature. Nuclei were stained with DAPI in mounting medium. Fluorescent images were taken with a Zeiss LSM-710 confocal laser scanning microscope.

### 2.11. Statistical analysis

All values were displayed as mean ± SD and statistical analysis was conducted using GrapdPad Prism 8 software. Comparisons between two groups were performed with Student's *t*-test, groups of three or more were analyzed by one-way ANOVA. *P* < 0.05 was considered as significant.

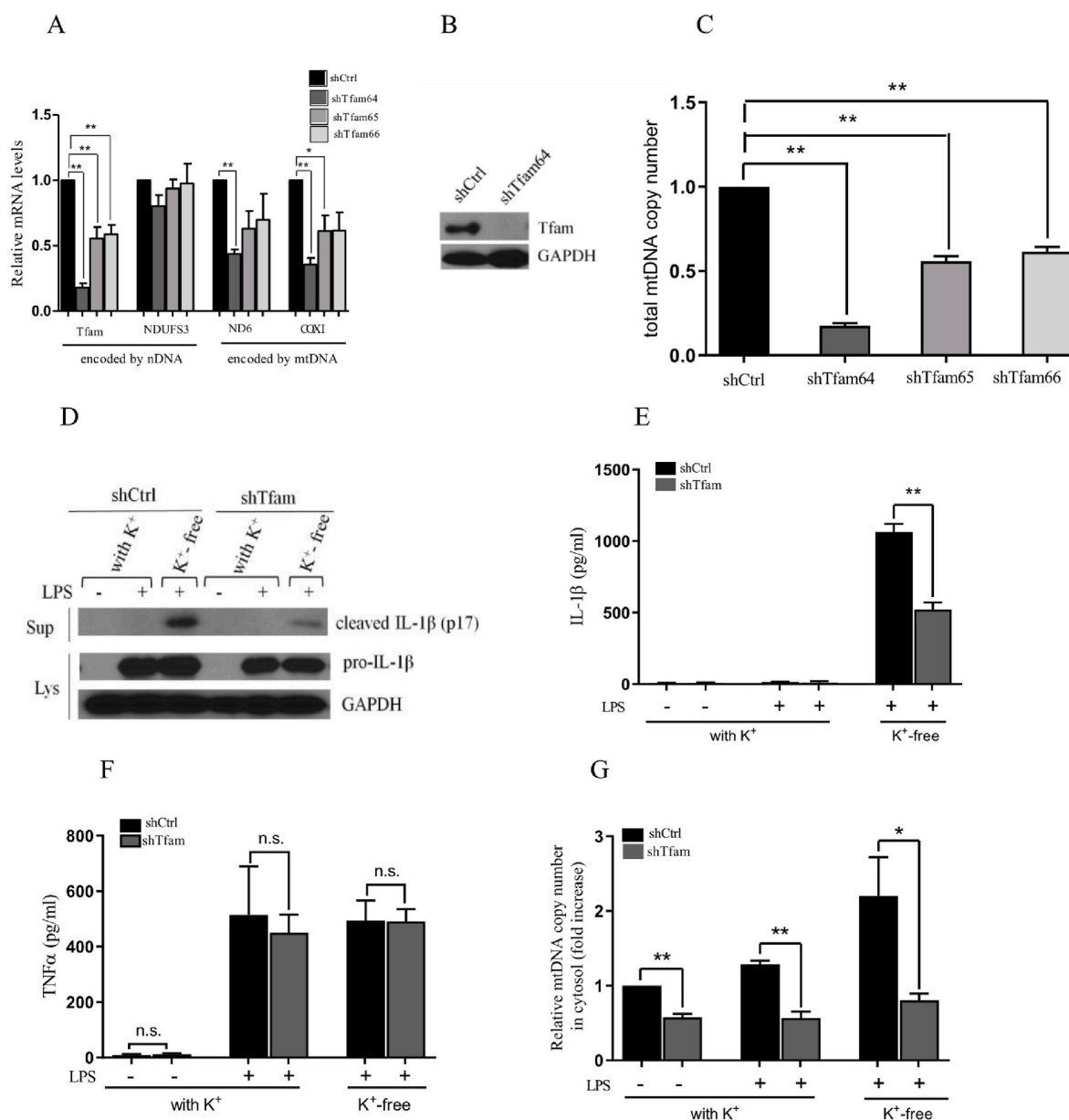


**Fig. 2.** Tfam knockdown leads to impaired NLRP3 inflammasome activation upon K<sup>+</sup>-efflux treatment. (A): The mRNA expressions of mitochondrial proteins encoded by nDNA and mtDNA genes in IBMMs were measured by qRT-PCR. (B): Tfam protein expression was detected by Western Blot. (C): Total mtDNA copy number in shCtrl and shTfam IBMMs was determined by qPCR. IBMMs were primed with 100 ng/ml LPS for 4 h, subsequently incubated with K<sup>+</sup> media or K<sup>+</sup>-free media for 2 h, (D): Cell lysates (Lys) and culture supernatant (Sup) were analyzed by Western Blot for IL-1β, (E, F): IL-1β and TNFα levels in culture media were detected by ELISA. (G) Cytosolic mtDNA copy number was determined by qPCR. n = 3, \**P* < 0.05, \*\**P* < 0.01.



### 3. Results

#### 3.1. Inflammatory state induced by LPS treatment in vitro leads to mitochondrial network expansion

Given the controversial role of mitochondria in NLRP3 inflammasome activation, we first interrogated whether mitochondria were required for NLRP3 inflammation activation or not. IBMMs and J774A.1, the two cell lines of mice macrophages, were treated with 100 ng/ml LPS in a time-dependent way to establish an in vitro inflammatory model based on previous established method [27]. As shown in Fig. 1, LPS treatment exhibited a significant increasing trend of mRNA expression for genes involved in mitochondrial biogenesis (Fig. 1A and B) and mitophagy (Fig. 1C and D) as the time extended. Accordingly, total copy number of mtDNA was also increased over time in response to LPS stimulation (Fig. 1E). Consistently, flow cytometry analysis showed increases of mitochondrial mass and mitochondrial membrane potential upon LPS treatment for 6 h and 24 h (Fig. 1F). These data, taken together, indicated that mitochondria were likely to be correlated with inflammatory responses. Moreover, LPS combined with ATP, a stimulus of NLRP3 inflammasome, also induced the mRNA expressions of genes involved in mitochondrial biogenesis (Fig. 1G) and mitophagy (Fig. 1H) significantly. Therefore, these data implied that mitochondria may be involved in inflammatory response, especially in the NLRP3 inflammasome activation process.

#### 3.2. Tfam knockdown leads to impaired NLRP3 inflammasome activation upon $K^+$ efflux treatment

Next, we investigated how mitochondria participate in NLRP3 inflammasome activation. As shown above, the mRNA expression of Tfam is significantly upregulated upon inflammation activation (Fig. 1A and B). Therefore, we set out to further validate the role of mitochondria in NLRP3 inflammasome activation by silencing Tfam using RNA interference (RNAi). We designed three shRNA sequences targeting Tfam, namely shTfam64, shTfam65 and shTfam66. As shown, the mRNA and protein expression of Tfam was effectively reduced by Tfam knockdown (Fig. 2A and B). Consistently, copy number of total mtDNA was significantly decreased, especially in shTfam64 group compared to shCtrl group (Fig. 2C). Moreover, Tfam knockdown induced a remarkable decrease of mRNA levels of NADH dehydrogenase (ND6) and cyclooxygenase I (COXI) which are encoded by mtDNA, whereas NADH: Ubiquinone Oxidoreductase Core Subunit S3 (NDUFS3), which is encoded by nDNA, did not differ from shCtrl group (Fig. 2A). Therefore, the macrophages treated with shTfam64, which have the highest silencing efficiency, were used in the following experiments. Given the fact that  $K^+$  efflux signaling is considered to be one of the common pathways through which various endogenous and exogenous agonists activate NLRP3, it prompted us to investigate whether the mitochondrial mechanism of NLRP3 inflammasome activation is depended on  $K^+$  efflux. Briefly, the macrophages were vehicle-treated or primed with LPS prior to  $K^+$  stimulation, then they were incubated in regular medium containing  $K^+$  or  $K^+$ -free medium in which  $K^+$  was replaced by  $Na^+$  to induce  $K^+$  efflux. Consistent with the previous study [14], we found that LPS combined with  $K^+$  efflux was sufficient to activate NLRP3 inflammasome in shCtrl cells (Fig. 2D), as reflected by induction of protein expression of cleaved IL-1 $\beta$  and secretion of IL-1 $\beta$  levels into culture medium (Fig. 2E). This can be explained by the reason that LPS, as one of the PAMPs, initiated the “priming” stage of NLRP3 inflammasome and then induced the generation of pro-IL-1 $\beta$ . By contrast, “ $K^+$  efflux”, as one of the agonists of NLRP3 inflammasome “activation” stage, led to pro-IL-1 $\beta$  cleavage to generate mature IL-1 $\beta$ . It is noteworthy that the NLRP3 inflammasome activation induced by  $K^+$  efflux in LPS-primed cells was markedly impaired by Tfam silencing (Fig. 2D and E). Moreover, the increased cytosolic release of mtDNA was observed in response to  $K^+$  efflux in LPS-primed cells, whereas the elevation in

release was suppressed by Tfam knockdown as well (Fig. 2G), while no significant change was observed in TNF $\alpha$  levels in response to Tfam knockdown, since it was produced in NLRP3-independent manner [18] (Fig. 2F). Taken together, these results suggested that mitochondria mediated NLRP3 inflammasome activation probably via regulating the cytosolic release of mtDNA, which is regulated by Tfam.

#### 3.3. The release of mtDNA into cytoplasm induced by $K^+$ efflux activates

##### 3.3.1. NLRP3 inflammasome

Although mitochondrial dysfunction resulted in the cytosolic release of mtDNA, which then binds to and activates NLRP3 inflammasome [22]. Yet little is known about the role of mtDNA in  $K^+$  efflux-induced NLRP3 inflammasome activation. As shown above, we found that the NLRP3 inflammasome activation induced by  $K^+$  efflux in LPS-primed cells was blunted by Tfam knockdown and was accompanied by reduction of cytosolic release of mtDNA, suggesting the involvement of mtDNA in  $K^+$  efflux-induced NLRP3 inflammasome activation in LPS-primed cells. However, multiple inflammatory responses, such as impaired oxidative phosphorylation (OXPHOS) and increased accumulation of mitochondrial damage [28], were altered by Tfam knockdown simultaneously besides mtDNA release. Therefore, to explore the specific role of mtDNA in NLRP3 inflammasome activation, we generated a cell line with mtDNA deficiency ( $\rho 0$  J774A.1 macrophage) by treating J774A.1 macrophages with EtBr. As previously reported, treatment with 100 ng/ml EtBr for 2 weeks led to a significant reduction of total mtDNA copy number [22,29] (Fig. 3A). Consistent with this, mtDNA deficiency resulted in reduced mRNA expressions of mtDNA-encoded mitochondrial proteins, ND6 and COX I, whereas no obvious effect was observed in nDNA-encoded mitochondrial proteins, peroxisome proliferator-activated receptor- $\gamma$  coactivator-1 $\alpha$  (PGC-1 $\alpha$ ) and NDUFS3 (Fig. 3B). Intriguingly, we found for the first time that the  $K^+$  efflux-induced NLRP3 inflammasome activation was significantly inhibited by mtDNA deficiency in LPS-primed cells (Fig. 3C and D). Similar to the result of Fig. 2F, the level of TNF $\alpha$  was not affected by mtDNA deficiency as it was produced in NLRP3-independent manner (Fig. 3E). The cytosolic release of mtDNA induced by  $K^+$  efflux was also inhibited by mtDNA deficiency in LPS-primed cells (Fig. 3F), whereas mtDNA deficiency had no obvious effect on  $K^+$  efflux (Fig. 3G). These data indicate that the cytosolic release of mtDNA induced by  $K^+$  efflux is sufficient to activate NLRP3 inflammasome. In line with these data, our immunofluorescence results showed that NLRP3 puncta was formed and translocated to mitochondria under  $K^+$  efflux induction in LPS-primed cells (Fig. 3H). Consistent with immunoblots and ELISA results, we further observed that NLRP3 could not form puncta when mtDNA was depleted in LPS-primed cells (Fig. 3H). These results, taken together, further confirmed that the cytosolic release of mtDNA induced by  $K^+$  efflux was prerequisite for activating NLRP3 inflammasome.

### 4. Discussion

Our study demonstrated that activation of inflammation induced the expression of genes involved in mitochondrial biogenesis and mitophagy and gradually led to increases in mitochondrial mass and mitochondrial membrane potential, suggesting an involvement of mitochondria in inflammatory responses. Furthermore, we demonstrated that inhibition of mitochondrial biogenesis by Tfam knockdown remarkably attenuated  $K^+$  efflux-induced NLRP3 inflammasome activation and this process was tightly associated with mtDNA. Indeed, we found that reduction of mtDNA by EtBr treatment reversed inflammasome activation induced by  $K^+$  efflux, which has been the major novel finding in this manuscript. Our study showed that mitochondrial DNA release induced by  $K^+$  efflux in macrophages activated NLRP3 inflammasome. Besides this, mtDNA release triggers NLRP3 inflammasome activation during infection by SFTS virus [30], atherosclerosis [31] and diabetes [32]. In summary, mtDNA may serve as potentially therapeutic target for NLRP3

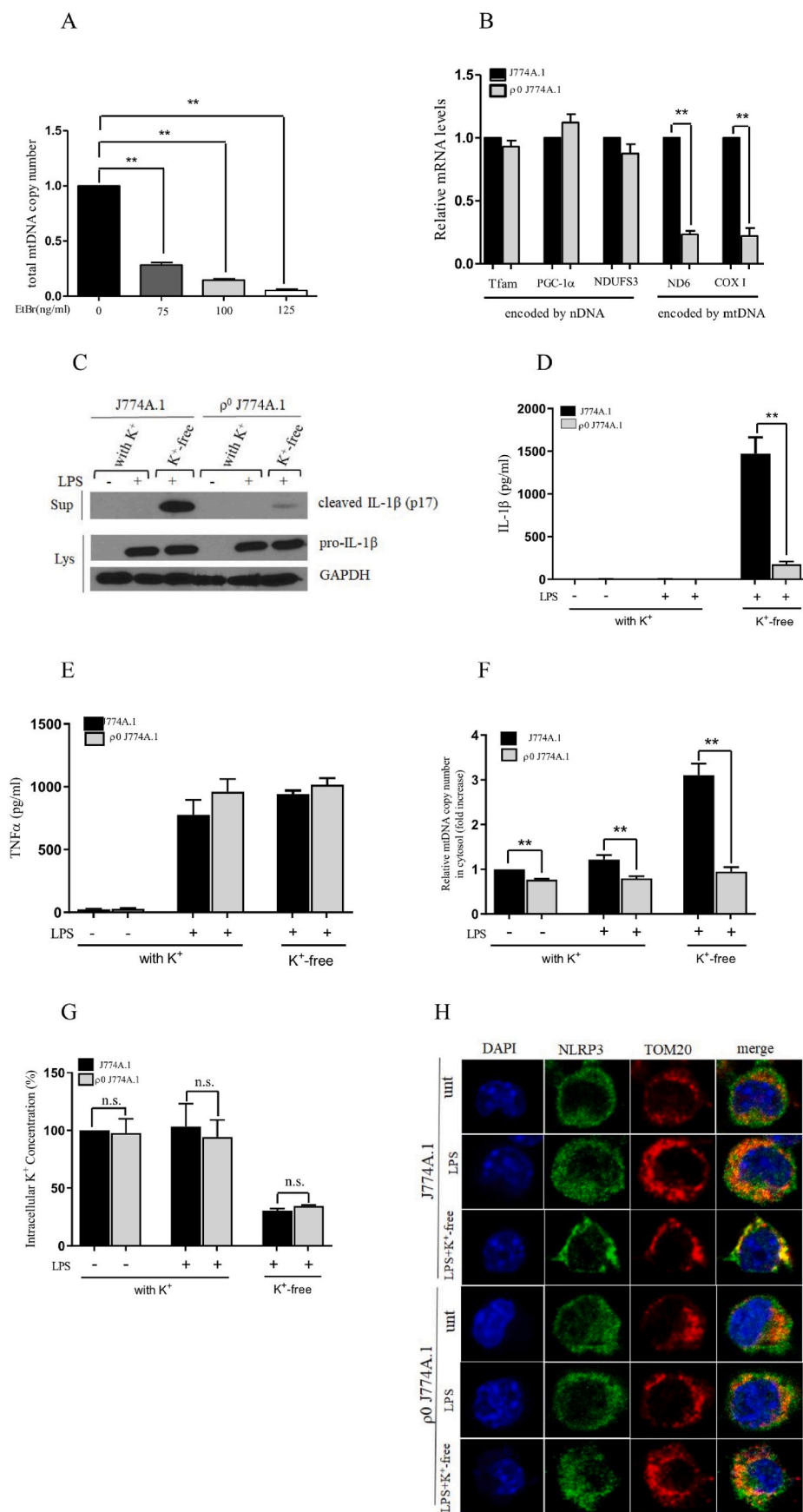


**Fig. 3.** The release of mtDNA into cytoplasm induced by K<sup>+</sup> efflux activates NLRP3 inflammasome. (A) J774A.1 macrophages were exposed to EtBr at indicated doses. Total mtDNA copy number was determined by qPCR. (B) Relative mRNA expression of genes encoded by nDNA and mtDNA were measured by qRT-PCR. (C) J774A.1 macrophages were vehicle-treated or primed with LPS for 4 h, followed by K<sup>+</sup> media or K<sup>+</sup>-free media incubation for 2 h. Cell lysates (lys) and culture supernatant (Sup) were analyzed by Western Blot for caspase-1 and IL-1β. (D, E) IL-1β and TNFα levels in culture media were analyzed by ELISA. (F) Relative mtDNA copy number in cytoplasm was measured by qPCR. (G) Intracellular K<sup>+</sup> concentration was measured by the potassium assay kit. (H) J774A.1 macrophages were analyzed for the activity and co-localization of NLRP3 with mitochondria (TOM20) using confocal microscopy (100X). n = 3, \*P < 0.05, \*\*P < 0.01.

inflammasome-related diseases if treated with agents that could lower cytosolic mtDNA release under pathological conditions.

So far, the NLRP3 inflammasome has been known to regulate a variety of metabolic disorders, for instance non-alcoholic steatopatitis (NASH), as blockade of NLRP3 inflammasome could reduce hepatic inflammation and fibrosis in murine NASH models [33]. Yet the specific mechanisms are still not clear. In the present study, we first observed increased mitochondrial biogenesis and mitophagy in the context of inflammation activation, possibly due to the biogenesis of mitochondria and clearance of damaged mitochondria were increased and served as a compensatory pathway to protect cells from excessive inflammation. In order to understand the molecular mechanism that mediating this process, we inhibited the expression of Tfam expression in macrophages since that Tfam is responsible for mtDNA transcription and replication but its potential role in NLRP3 inflammasome activation is rarely reported. Here we found that Tfam knockdown also blunted  $K^+$  efflux-induced NLRP3 inflammasome activation. Moreover, the increased release of mtDNA into cytosol induced by  $K^+$  efflux was suppressed upon Tfam knockdown, indicating that  $K^+$  efflux is sufficient but not necessary for NLRP3 inflammasome activation. By contrast, mtDNA released into cytosol induced by  $K^+$  efflux was involved in NLRP3 inflammasome activation. Taken together, these results suggested that mitochondria participated in NLRP3 inflammasome activation probably via regulating the cytosolic release of mtDNA, which is Tfam-dependent.

Compared to nucleus, mitochondria have a relatively independent replication and transcription machinery for its own genome, namely mtDNA. Recent studies have shown that mtDNA, as one of the intracellular DAMPs, is released into cytosol after mitochondrial damage and then activates NLRP3 inflammasome by interacting with it [22,23]. Yet little is known about the role of mtDNA in  $K^+$  efflux-induced NLRP3 inflammasome activation, meanwhile, the release of mtDNA into cytosol induced by  $K^+$  efflux was robustly blunted by mtDNA deficiency without affecting  $K^+$  efflux. Taken together, these findings indicate that the release of mtDNA into cytosol is under control of  $K^+$  efflux for activating NLRP3 inflammasome. Additionally, previous studies showed that NLRP3 was mainly localized in the endoplasmic reticulum or cytoplasm, instead of distribution in mitochondria, Golgi and lysosome in basal condition. Yet once activated, NLRP3 was translocated and redistributed on mitochondria and mitochondria-associated endoplasmic reticulum membranes (MAMS) [20,34,35]. In line with these data, we also observed that NLRP3 inflammasome was activated and translocated to mitochondria in response to  $K^+$  efflux induction. However, there are conflicting results in terms of the subcellular location of NLRP3 upon stimulation, as evidence by other studies that the interfaces between the Golgi apparatus and endoplasmic reticulum may be the central nexus for NLRP3 inflammasome activation [36,37], especially one recent study have demonstrated that the Golgi, not mitochondria served as the platform for NLRP3 inflammasome activation [24]. The discrepancies may be partially due to the diversity of NLRP3 agonists and more studies are needed to address this question.

The strength of the study is the cross-talk between NLRP3 inflammasome activation and mitochondria. Our data suggest that inflammation activation leads to expansion of mitochondrial network, which likely fuels inflammation, as blockade of this expansion blunts NLRP3 inflammasome activation (Fig. 4). We demonstrated that the cytosolic release of mtDNA induced by  $K^+$  efflux in macrophages activates NLRP3 inflammasome and raises the possibility that dysregulated mitochondria as a therapeutic target for NLRP3 inflammasome-regulated diseases [7, 38–40].

#### Data availability

The authors can provide the data of this research article on request.

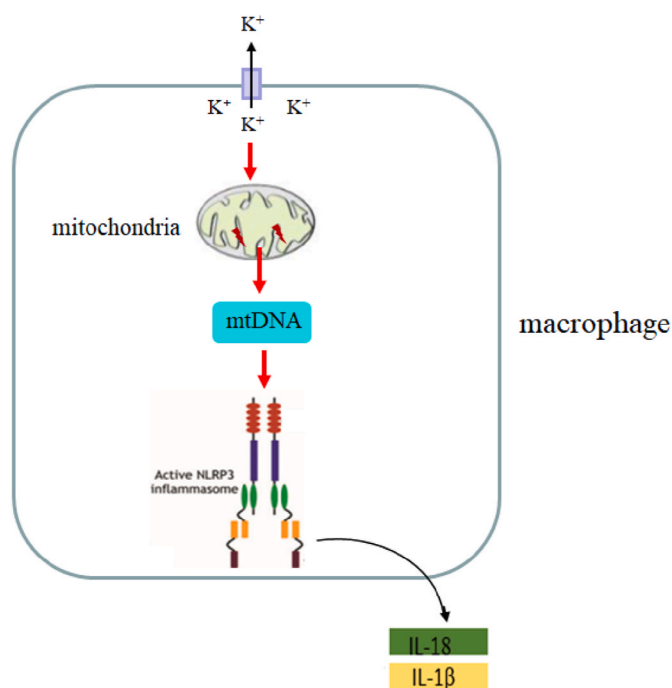


Fig. 4. Work model: Intracellular  $K^+$  efflux causes the release of mtDNA into cytosol, then activates NLRP3 inflammasome.

#### CRediT authorship contribution statement

**Tan Zhang:** Project Designation, Data Acquisition, Funding acquisition, Formal analysis, Writing – original draft, Review & Editing, Writing – review & editing. **Jingyao Zhao:** Investigation, Supervision. **Tiemin Liu:** Writing – review & editing. **Wei Cheng:** Editing, Writing – review & editing, Supervision. **Yibing Wang:** Writing – review & editing, Supervision. **Shuzhe Ding:** Funding acquisition, Supervision, Writing – review & editing. **Ru Wang:** Funding acquisition, Supervision, Writing – review & editing.

#### Declaration of competing interest

The authors declare no conflict of interest.

#### Acknowledgements

We thank all the members in the labs for valuable help. We also thank Dr. Ru Wang and Dr. Shuzhe Ding for proposing and supporting this project. We thank Dr. Sankar Ghosh (Columbia University, Vagelos College of Physicians & Surgeons, New York, USA) for hosting Tan Zhang and supporting this research. This work was supported by the National Natural Science Foundation of China (31971097) to Dr. Ru Wang, the National Natural Science Foundation of China (31671241) to Dr. Shuzhe Ding and by institutional funds from Columbia University to Dr. Sankar Ghosh.

#### References

- [1] Gong T, Liu L, Jiang W, et al. DAMP-sensing receptors in sterile inflammation and inflammatory diseases[J]. *Nat Rev Immunol* 2020;20(2):95–112.
- [2] Martinon F, Burns K, Tschopp J. The inflammasome: a molecular platform triggering activation of inflammatory caspases and processing of proIL-beta[J]. *Mol Cell* 2002;10(2):417–26.
- [3] Hoffman HM, Mueller JL, Broide DH, et al. Mutation of a new gene encoding a putative pyrin-like protein causes familial cold autoinflammatory syndrome and Muckle-Wells syndrome[J]. *Nat Genet* 2001;29(3):301–5.
- [4] Moossavi M, Parsamanesh N, Bahrami A, et al. Role of the NLRP3 inflammasome in cancer[J]. *Mol Cancer* 2018;17(1):158.



- [5] Lee HM, Kim JJ, Kim HJ, et al. Upregulated NLRP3 inflammasome activation in patients with type 2 diabetes[J]. *Diabetes* 2013;62(1):194–204.
- [6] Rheinheimer J, de Souza BM, Cardoso NS, et al. Current role of the NLRP3 inflammasome on obesity and insulin resistance: a systematic review[J]. *Metabolism* 2017;74:1–9.
- [7] Rovira-Llopis S, Apostolova N, Banuls C, et al. Mitochondria, the NLRP3 inflammasome, and sirtuins in type 2 diabetes: new therapeutic targets[J]. *Antioxidants Redox Signal* 2018;29(8):749–91.
- [8] Mridha AR, Wree A, Robertson A, et al. NLRP3 inflammasome blockade reduces liver inflammation and fibrosis in experimental NASH in mice[J]. *J Hepatol* 2017; 66(5):1037–46.
- [9] So AK, Martinon F. Inflammation in gout: mechanisms and therapeutic targets[J]. *Nat Rev Rheumatol* 2017;13(11):639–47.
- [10] Baldrighi M, Mallat Z, Li X. NLRP3 inflammasome pathways in atherosclerosis[J]. *Atherosclerosis* 2017;267:127–38.
- [11] Ising C, Venegas C, Zhang S, et al. NLRP3 inflammasome activation drives tau pathology[J]. *Nature* 2019;575(7784):669–73.
- [12] Swanson KV, Deng M, Ting JP. The NLRP3 inflammasome: molecular activation and regulation to therapeutics[J]. *Nat Rev Immunol* 2019;19(8):477–89.
- [13] Zhen Y, Zhang H. NLRP3 inflammasome and inflammatory bowel disease[J]. *Front Immunol* 2019;10:276.
- [14] Munoz-Planillo R, Kuffa P, Martinez-Colon G, et al. (+) efflux is the common trigger of NLRP3 inflammasome activation by bacterial toxins and particulate matter[J]. *Immunity* 2013;38(6):1142–53.
- [15] Di A, Xiong S, Ye Z, et al. The TWIK2 potassium efflux channel in macrophages mediates NLRP3 inflammasome-induced inflammation[J]. *Immunity* 2018;49(1): 56–65.
- [16] Murakami T, Ockinger J, Yu J, et al. Critical role for calcium mobilization in activation of the NLRP3 inflammasome[J]. *Proc Natl Acad Sci U S A* 2012;109(28): 11282–7.
- [17] Lee GS, Subramanian N, Kim AI, et al. The calcium-sensing receptor regulates the NLRP3 inflammasome through Ca<sup>2+</sup> and cAMP[J]. *Nature* 2012;492(7427): 123–7.
- [18] Tang T, Lang X, Xu C, et al. CLICs-dependent chloride efflux is an essential and proximal upstream event for NLRP3 inflammasome activation[J]. *Nat Commun* 2017;8(1):202.
- [19] Hornung V, Bauernfeind F, Halle A, et al. Silica crystals and aluminum salts activate the NALP3 inflammasome through phagosomal destabilization[J]. *Nat Immunol* 2008;9(8):847–56.
- [20] Zhou R, Yazdi AS, Menu P, et al. A role for mitochondria in NLRP3 inflammasome activation[J]. *Nature* 2011;469(7329):221–5.
- [21] Hughes MM, O'Neill L. Metabolic regulation of NLRP3[J]. *Immunol Rev* 2018;281 (1):88–98.
- [22] Nakahira K, Haspel JA, Rathinam VA, et al. Autophagy proteins regulate innate immune responses by inhibiting the release of mitochondrial DNA mediated by the NALP3 inflammasome[J]. *Nat Immunol* 2011;12(3):222–30.
- [23] Shimada K, Crother TR, Karlin J, et al. Oxidized mitochondrial DNA activates the NLRP3 inflammasome during apoptosis. [J]. *Immunity*. 2012;36(3):401–14.
- [24] Chen J, Chen ZJ. PtdIns4P on dispersed trans-Golgi network mediates NLRP3 inflammasome activation[J]. *Nature* 2018;564(7734):71–6.
- [25] Ngo HB, Lovely GA, Phillips R, et al. Distinct structural features of TFAM drive mitochondrial DNA packaging versus transcriptional activation[J]. *Nat Commun* 2014;5:3077.
- [26] Carneiro F, Lepelley A, Seeley JJ, et al. An essential role for ECSIT in mitochondrial complex I assembly and mitophagy in macrophages[J]. *Cell Rep* 2018;22(10): 2654–66.
- [27] Tan RZ, Liu J, Zhang YY, et al. Curcumin relieved cisplatin-induced kidney inflammation through inhibiting Mincle-maintained M1 macrophage phenotype [J]. *Phytomedicine* 2019;52:284–94.
- [28] Zhou X, Trinh-Minh T, Tran-Manh C, et al. Impaired TFAM expression promotes mitochondrial damage to drive fibroblast activation and fibrosis in systemic sclerosis[J]. *Arthritis Rheumatol* 2021.
- [29] Hashiguchi K, Zhang-Akiyama QM. Establishment of human cell lines lacking mitochondrial DNA[J]. *Methods Mol Biol* 2009;554:383–91.
- [30] Li S, Li H, Zhang YL, et al. SFTSV infection induces BAK/BAX-Dependent mitochondrial DNA release to trigger NLRP3 inflammasome activation[J]. *Cell Rep* 2020;30(13):4370–85.
- [31] Li D, Yang S, Xing Y, et al. Novel insights and current evidence for mechanisms of atherosclerosis: mitochondrial dynamics as a potential therapeutic target[J]. *Front Cell Dev Biol* 2021;9:673839.
- [32] Pereira CA, Carlos D, Ferreira NS, et al. Mitochondrial DNA promotes NLRP3 inflammasome activation and contributes to endothelial dysfunction and inflammation in type 1 diabetes[J]. *Front Physiol* 2019;10:1557.
- [33] Mridha AR, Wree A, Robertson A, et al. NLRP3 inflammasome blockade reduces liver inflammation and fibrosis in experimental NASH in mice[J]. *J Hepatol* 2017; 66(5):1037–46.
- [34] Subramanian N, Natarajan K, Clatworthy MR, et al. The adaptor MAVS promotes NLRP3 mitochondrial localization and inflammasome activation[J]. *Cell* 2013;153 (2):348–61.
- [35] Misawa T, Takahama M, Kozaki T, et al. Microtubule-driven spatial arrangement of mitochondria promotes activation of the NLRP3 inflammasome[J]. *Nat Immunol* 2013;14(5):454–60.
- [36] Zhang Z, Meszaros G, He WT, et al. Protein kinase D at the Golgi controls NLRP3 inflammasome activation[J]. *J Exp Med* 2017;214(9):2671–93.
- [37] Guo C, Chi Z, Jiang D, et al. Cholesterol homeostatic regulator SCAP-SREBP2 integrates NLRP3 inflammasome activation and cholesterol biosynthetic signaling in macrophages[J]. *Immunity* 2018;49(5):842–56.
- [38] Li Y, Xia Y, Yin S, et al. Targeting microglial alpha-synuclein/TLRs/NF-kappaB/NLRP3 inflammasome Axis in Parkinson's disease[J]. *Front Immunol* 2021;12: 719807.
- [39] Deng Y, Xie M, Li Q, et al. Targeting mitochondria-inflammation circuit by beta-hydroxybutyrate mitigates HFpEF[J]. *Circ Res* 2021;128(2):232–45.
- [40] Wu AG, Zhou XG, Qiao G, et al. Targeting microglial autophagic degradation in NLRP3 inflammasome-mediated neurodegenerative diseases[J]. *Ageing Res Rev* 2021;65:101202.